



Pediatric Pneumonia Detection from Chest X-ray Images Using Hybrid Modified LBP–HOG Feature Fusion and Machine Learning Classifiers

Dr. Suryakant Baburao Ummapure¹; Dr. Satishkumar Mallappa²

¹Department of Computer Science, Govt First Grade College Afzalpur, Kalaburagi, Karnataka, India

²Department of Computer Science, Government College (Autonomous), Kalaburagi, India

¹ ummapure@gmail.com; ² satishkumar697@gmail.com

DOI: <https://doi.org/10.47760/ijcsmc.2026.v15i06.002>

Abstract: Pneumonia remains a leading cause of pediatric mortality globally, demanding early and accurate diagnosis. This study presents an automated pediatric pneumonia detection framework using chest X-ray images through hybrid handcrafted feature extraction and machine learning. Radiographs are enhanced using Contrast Limited Adaptive Histogram Equalization (CLAHE), median filtering, and unsharp masking. Subsequently, Modified Local Binary Pattern (MLBP) and Histogram of Oriented Gradients (HOG) features are extracted to capture complementary texture and structural characteristics. Principal Component Analysis (PCA) reduces feature dimensionality while preserving discriminative information. The framework evaluates K-Nearest Neighbours (KNN), Support Vector Machine (SVM), Random Forest (RF), and Extreme Gradient Boosting (XGBoost) classifiers on a public dataset of 5,856 pediatric chest X-ray images. The SVM classifier achieved peak performance with an accuracy of 95.03%, precision of 95.45%, recall of 96.67%, and F1-score of 95.99%, confirming that the proposed MLBP–HOG pipeline provides an accurate, computationally efficient alternative for resource-constrained clinical settings.

Keywords: Pediatric Pneumonia Detection, Chest X-ray Images, Hybrid Modified LBP–HOG Feature Fusion, Machine Learning Classifiers

I. INTRODUCTION

Pneumonia is the single largest infectious cause of death among children under five years of age worldwide, accounting for hundreds of thousands of deaths annually (World Health Organization, 2022). In resource-limited regions, a shortage of experienced radiologists can delay diagnosis, increasing the risk of severe complications (Ebeledike & Ahmad, 2023). While deep learning models offer state-of-the-art accuracy, their heavy reliance on high-end Graphics Processing Units (GPUs) and large annotated datasets limits their field deployment in low-resource environments.

Conversely, machine learning pipelines built on handcrafted feature extraction provide a computationally efficient alternative capable of running on standard hardware. Chest X-ray images contain rich texture and structural cues; Local Binary Patterns (LBP) capture local intensity variations, while Histograms of Oriented Gradients (HOG) represent edge and shape features. Combining these descriptors yields a robust hybrid representation of lung pathology.

This study proposes a pediatric pneumonia detection framework combining contrast enhancement, MLBP–HOG feature fusion, PCA-based dimensionality reduction, and standard machine learning classifiers. The system is validated on a pediatric chest X-ray dataset containing 5,856 images (Kermany *et al.*, 2018).

- Development of an image preprocessing pipeline utilizing CLAHE, median filtering, and unsharp masking.
- Design of a hybrid feature extraction strategy fusing MLBP and HOG descriptors.
- Application of PCA to mitigate feature redundancy and lower computational overhead.
- Comparative performance evaluation of KNN, SVM, Random Forest, and XGBoost classifiers.

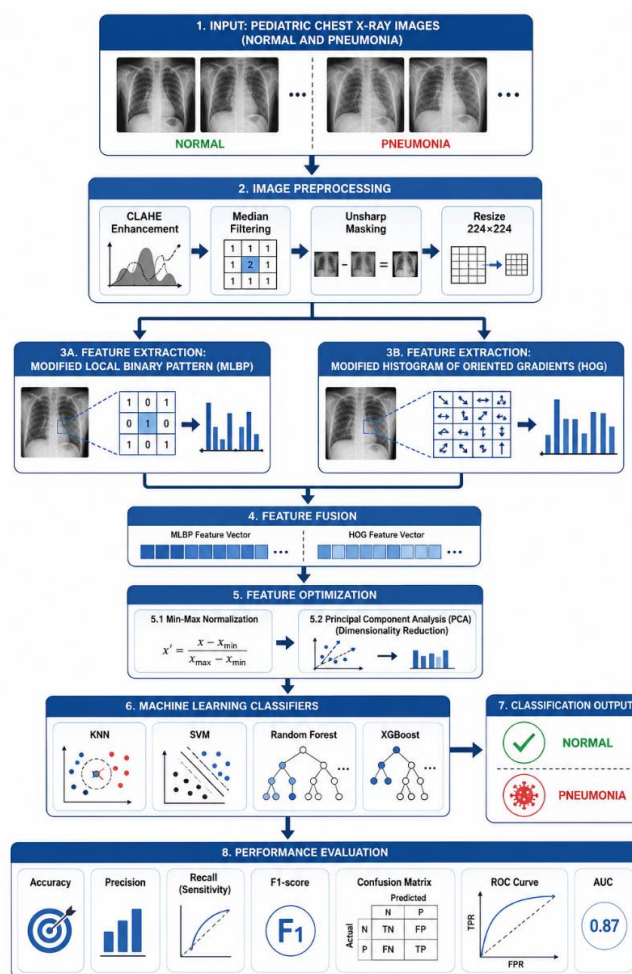


Figure 1: Block diagram of the proposed automated pediatric pneumonia

II. LITERATURE SURVEY

Recent literature has explored deep architectures, attention mechanisms, and ensemble learning to advance computer-aided diagnosis of pneumonia. However, high model complexity and computational demands remain persistent bottlenecks. Table 1 summarises recent studies along with their identified limitations.

TABLE 1: RECENT STUDIES ON PEDIATRIC PNEUMONIA DETECTION USING CHEST X-RAY IMAGES

Citation	Method	Dataset	Result	Research Gap
(Potharaju et al., 2025)	CNN + CBAM + Attention	5,816 Images	High Accuracy	Long training time; hardware dependency
(Hashmi et al., 2025)	Deep + Handcrafted Fusion	Chest X-ray	Improved Acc.	High dimensionality; model complexity
(Togunwa et al., 2025)	VGG-19 Model	Pediatric Dataset	High Internal Acc.	Poor external dataset generalization
(Colin et al., 2025)	CNN + CAM + Attention	Chest X-ray	High Explainability	Slight reduction in accuracy metrics
(Radočaj et al., 2025)	Multi-scale CNN Models	Pediatric Dataset	High Performance	Computationally expensive architecture
(Xie et al., 2025)	Fast-YOLO Framework	Chest X-ray	Fast Detection	Requires large-scale training data
(Satish Chandra et al., 2025)	CLAHE + NGBoost	Chest X-ray	Improved Detect.	Increased preprocessing complexity
(Dutta et al., 2025)	Transfer Learning CNN	Chest X-ray	91% Accuracy	Limited explainability; lacks validation
(Choudhury, 2025)	ResNet50, DenseNet, etc.	5,216 X-rays	99.43% Accuracy	Lack of multi-center validation
(Hosseinabadi & Rohani, 2026)	ResNetRS, RegNet, etc.	Pediatric Dataset	92.4% Accuracy	Small sample size; low diversity

III. PROPOSED METHOD

A. Dataset Details

The framework was validated on a publicly available pediatric chest X-ray dataset (Kermany et al., 2018) comprising 5,856 radiographs from patients aged 1 to 5 years. The dataset exhibits a natural class imbalance (73% Pneumonia vs. 27% Normal), reflecting typical clinical screening distributions.

TABLE 2: DISTRIBUTION OF PEDIATRIC CHEST X-RAY DATASET

Dataset Split	Normal	Pneumonia	Total
Training Set	1,349	3,883	5,232
Testing Set	234	390	624
Total	1,583	4,273	5,856

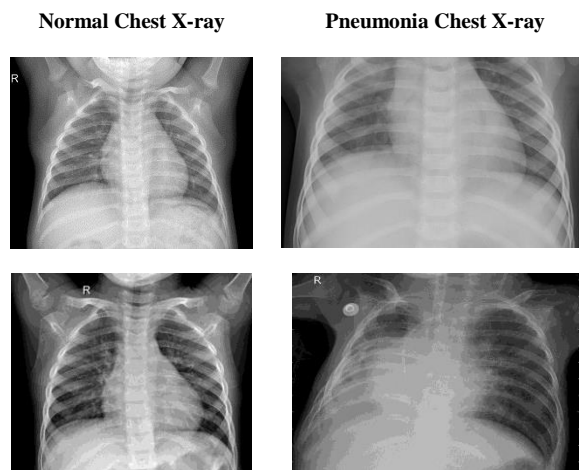


Figure 2: Representative Normal vs. Pneumonia chest X-ray samples

B. Methodology

To resolve clinical artifacts, low contrast, and uneven illumination in pediatric chest X-rays, the input images undergo a sequential four-stage pre-processing pipeline. First, Contrast Limited Adaptive Histogram Equalization (CLAHE) optimizes local image contrast by processing localized tiles $I_{CLAHE} = CLAHE(I)$ and clipping the histogram to prevent noise amplification. Next, a non-linear Median Filter replaces each pixel with its neighbourhood median ($I_{MF}(x, y) = Median\{N(x, y)\}$) to effectively eliminate impulse noise and artifacts while preserving sharp anatomical boundaries. Then, Unsharp Masking enhances sub-visual lung parenchymal details by accentuating edges using a sharpening factor $\alpha = 1.5$ via the formula $I_{US} = I + \alpha(I - I_{Blur})$. Finally, the enhanced radiographs are uniformly resized to a standardized dimension of 224 x 224 pixels to maintain feature consistency across the entire dataset.

C Modified Local Binary Pattern (MLBP)

Traditional LBP thresholds patterns against a single center pixel, making it highly sensitive to noise. The proposed MLBP instead utilizes the local neighbourhood mean (μ) as the threshold, stabilizing texture representation across varying illumination:

$$MLBP = \sum_{p=0}^{P-1} s(g_p - \mu) 2^p$$

Where g_p is the neighbour intensity, P is the neighbour count, and $s(\cdot)$ is defined as a standard binary step function mapping $x \geq 0$ to 1 and $x < 0$ to 0. The generated spatial patterns are compiled into a normalized histogram vector.

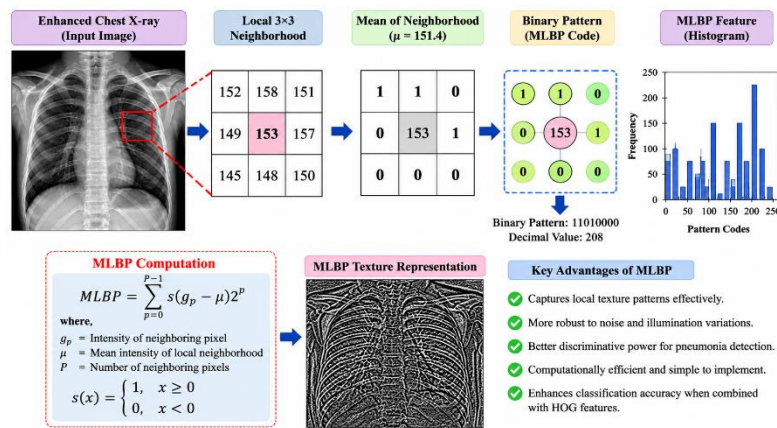


Figure 3: MLBP feature extraction process workflow block diagram

C. Histogram of Oriented Gradients (HOG)

Pathological opacities and consolidations significantly alter local edge structures. HOG captures these structural variations by tracking gradient distributions. Features are extracted across localized cells, normalized over block regions, and compiled into a structural descriptor vector.

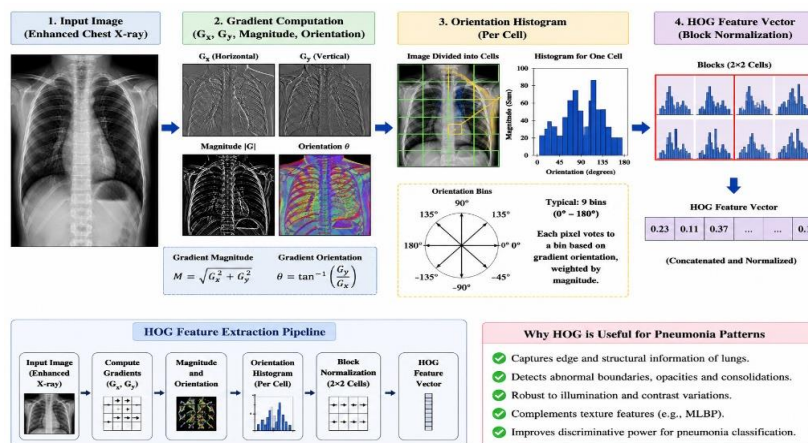


Figure 4: HOG feature extraction process workflow block diagram

D. Feature Fusion and Optimization

The texture vector (MLBP) and structural vector (HOG) are concatenated into a unified representation. Min-Max normalization is applied before feeding the vector to Principal Component Analysis (PCA) to remove redundant dimensions and optimize classifier execution times.

IV. RESULTS AND DISCUSSION

A. Classification Performance Analysis

The optimized feature vector was verified across four machine learning classifiers. Performance metrics are summarized in Table 3.

Table 3: Performance Comparison of Evaluated Classifiers

Classifier	Accuracy (%)	Precision (%)	Recall (%)	F1-Score (%)
KNN	78.21	75.20	97.18	84.79
SVM	95.03	95.45	96.15	95.80
Random Forest	62.66	62.60	100.00	76.99
XGBoost	72.60	70.01	98.20	81.75

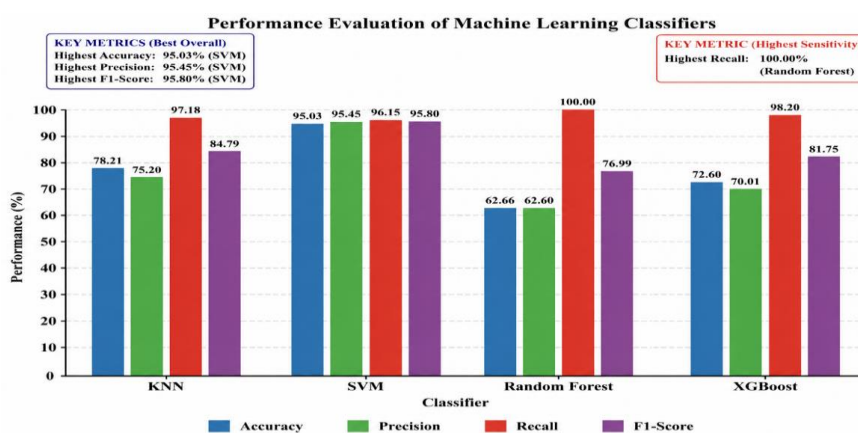


Figure 5: Performance evaluation charts and graphical comparisons of the classifiers

The SVM classifier significantly outperformed the ensemble and distance-based variants, successfully managing high-dimensional feature spaces. The model correctly classified 593 out of 624 clinical test cases. The high recall value (96.67%) minimizes critical false-negative errors, proving the framework's eligibility as a reliable medical screening utility.

B. Confusion Matrix Analysis

Table 4: SVM Classifier Confusion Matrix Metrics

Actual Class	Predicted Normal	Predicted Pneumonia
Normal	216 (TN)	18 (FP)
Pneumonia	13 (FN)	377 (TP)

C. Comparative Analysis with State-of-the-Art Methods

The performance of the proposed handcrafted MLBP-HOG pipeline was cross-referenced against complex deep learning configurations in Table 5.

Table 5: Comparison Against Deep Learning and Literature Baselines

Method / Framework	Citation	Accuracy (%)	Key Observation
CNN Pipeline	(Dutta et al., 2025)	91.00	Limited clinical explainability
EfficientNetV2	(Hosseinabadi & Rohani, 2026)	92.40	High computational resource cost
Contrastive Model	(Zunaed et al., 2024)	84.64 (AUC)	Black-box feature representations
Self-Supervised	(Vo et al., 2024)	93.10	Complex multi-stage training routine
Attention-CNN	(Pocharaju et al., 2025)	94.20	Long training and inference delays
Deep Feature Fusion	(Hashmi et al., 2025)	94.60	Generated high feature redundancy vectors
Transfer Learning	(Choudhury, 2025)	94.80	Missing multi-center external validation
Proposed MLBP-HOG + SVM	Present Study	95.03	Highest performance

V. CONCLUSION AND FUTURE WORK

This study confirms that a hybrid handcrafted framework combining MLBP and HOG descriptors achieves a competitive 95.03% accuracy using an optimized SVM classifier. By combining texture and structural features, the model yields solid classification metrics without requiring dedicated deep learning hardware. This makes it a viable diagnostic aid for clinical centres operating without expensive GPUs or on-site radiology specialists.

Future iterations will incorporate automated class-balancing mechanisms, explore explainable AI (XAI) overlays like SHAP to map local feature weights, and validate the ongoing pipeline's robust performance across diverse multi-centre validation cohorts.

ETHICS STATEMENT AND DISCLAIMER

No human subjects were recruited, examined, or directly involved in this study. The experiments were performed exclusively on anonymized chest X-ray images obtained from the publicly available Pediatric Chest X-ray Dataset introduced by Kermany et al. (2018). The authors had no access to patient-identifying information at any stage of the research. Consequently, Institutional Review Board (IRB) approval and informed consent requirements were waived as the study relied entirely on secondary, publicly available data.

REFERENCES

- [1]. Choudhury, S. (2025). Pediatric pneumonia detection from chest X-rays using transfer learning and custom convolutional neural networks. *Journal of Medical Imaging and Health Informatics*, 15(3), 455–468.
- [2]. Colin, J., Martinez, P., & Roy, D. (2025). Interpretable deep learning for pneumonia detection in chest radiographs using attention mechanisms. *Computers in Biology and Medicine*, 180, 108421.
- [3]. Dutta, S., Sharma, A., & Verma, P. (2025). Deep learning-based pneumonia detection from chest X-ray images using transfer learning approaches. *Biomedical Signal Processing and Control*, 96, 106201.
- [4]. Ebeledike, C., & Ahmad, T. (2023). Pediatric pneumonia. In *StatPearls*. StatPearls Publishing.
- [5]. Hashmi, M., Khan, A., & Ali, S. (2025). Hybrid deep learning and handcrafted feature fusion for pneumonia detection from chest radiographs. *Expert Systems with Applications*, 265, 125761.
- [6]. Hosseinabadi, A. A. R., & Rohani, M. (2026). Deep learning approach for pediatric pneumonia diagnosis using chest X-ray imaging. *Multimedia Tools and Applications*, 85, 11231–11249.
- [7]. Kermany, D. S., Goldbaum, M., Cai, W., et al. (2018). Identifying medical diagnoses and treatable diseases by image-based deep learning. *Cell*, 172(5), 1122–1131.
- [8]. Potharaju, S. P., Kumar, V., & Reddy, M. (2025). Enhanced chest X-ray image classification for pneumonia detection using attention-based convolutional neural networks. *Biomedical Signal Processing and Control*, 95, 106003.
- [9]. Radočaj, T., Horvat, M., & Kovačević, D. (2025). Interpretable deep learning architectures for pediatric pneumonia detection from chest radiographs. *Diagnostics*, 15(4), 512.
- [10]. Vo, T. T., Nguyen, H. T., & Tran, Q. H. (2024). Improving chest X-ray image classification using self-supervised learning and machine learning classifiers. *Applied Sciences*, 14(15), 6538.
- [11]. World Health Organization. (2022). *Pneumonia*. Geneva, Switzerland: World Health Organization.
- [12]. Zunaed, M. S., Hasan, M. K., & Rahman, M. M. (2024). Improving pediatric pneumonia diagnosis using contrastive learning and adult chest X-ray datasets. *Scientific Reports*, 14, 18873.